Tree-ring isotopes from the Swiss Alps reveal non-climatic fingerprints of cyclic insect population outbreaks over the past 700 years

Short title: Isotopes as non-climatic fingerprints

Vitali, Valentina *[1], Peters, Richard L. [2], Lehmann, Marco M. [1], Leuenberger, Markus [3], Treydte, Kerstin [4], Büntgen, Ulf [4,5,6,7], Schuler, Philipp [1], Saurer, Matthias [1]

[1] Stable Isotope Research Centre (SIRC), Ecosystem Ecology, Forest Dynamics, Swiss Federal Institute for Forest, Snow and Landscape Research WSL, CH-8903 Birmensdorf, Switzerland

[2] Physiological Plant Ecology, Department of Environmental Sciences, University of Basel, Schönbeinstrasse 6, CH-4056 Basel, Switzerland

[3] Climate and Environmental Physics Division and Oeschger Centre for Climate Change Research, University of Bern, Sidlerstrasse 5, CH-3012 Bern, Switzerland

[4] Dendrosciences, Forest Dynamics, Swiss Federal Institute for Forest, Snow and Landscape Research WSL, CH-8903, Birmensdorf, Switzerland

[5] Department of Geography, University of Cambridge, Downing Place, CB2 3EN Cambridge, UK

[6] Global Change Research Institute (CzechGlobe), Czech Academy of Sciences, 603 00 Brno, Czech Republic

[7] Department of Geography, Faculty of Science, Masaryk University, 611 37 Brno, Czech Republic

Funding information: This study was supported by the Swiss National Science Foundation (SNSF) with the following projects. VV, MS: SNSF project No.200020_182092., RLP: SNSF grant No. P2BSP3_184475, MML: SNSF project No. 179978, KT: SNSF project No. 200021_175888.

Address: Swiss Federal Institute for Forest, Snow and Landscape Research WSL, Zürcherstrasse 111, CH-8903 Birmensdorf, Switzerland

Corresponding author's e-mail address: *valentina.vitali@wsl.ch; ORCiD: orcid.org/0000-0002-3045-6178

Keywords: dendroecology, deuterium, ecophysiology, insect defoliation, insect outbreak, plant-pathogen interaction, stable isotope, tree physiology, tree-ring cellulose, *Zeiraphera griseana*

Abstract

Recent experiments have underlined the potential of δ^2H in tree-ring cellulose as a physiological indicator of shifts in autotrophic versus heterotrophic processes (i.e. the use of fresh versus stored non-structural carbohydrates). However, the impact of these processes has not yet been quantified under

natural conditions. Defoliator outbreaks disrupt tree functioning and carbon assimilation, stimulating remobilization, therefore providing a unique opportunity to improve our understanding of changes in δ^2H. By exploring a 700-year tree-ring isotope chronology from Switzerland, we assessed the impact of 79 larch budmoth (LBM, *Zeiraphera griseana*) outbreaks on the growth of its host tree species, *Larix decidua*.

LBM outbreaks significantly altered the tree-ring isotopic signature, creating a ^2H-enrichment and an ^{18}O- and ^{13}C-depletion. Changes in tree physiological functioning in outbreak years are shown by the decoupling of δ^2H and $\delta^{18}O$ (O–H relationship), in contrast to the positive correlation in non-outbreak years. Across the centuries, the O–H relationship in outbreak years was not significantly affected by temperature, indicating that non-climatic physiological processes dominate over climate in determining δ^2H. We conclude that the combination of these isotopic parameters can serve as a metric for assessing changes in physiological mechanisms over time.

1. Introduction

The isotopic ratio of the non-exchangeable carbon-bound hydrogen (δ^2H) has rarely been studied in tree-ring cellulose ($C_6H_{10}O_5$), while carbon ($\delta^{13}C$) and oxygen ($\delta^{18}O$) isotopes in tree rings have been used extensively to investigate the effects of past climatic conditions (Saurer *et al.*, 1995; Saurer, Aellen & Siegwolf, 1997; Loader *et al.*, 2007; Andreu-Hayles *et al.*, 2017; Sakashita *et al.*, 2018; Loader *et al.*, 2020; Shestakova & Martínez-Sancho, 2021; Field *et al.*, 2022; Sano *et al.*, 2022). The climatic signal of ^2H has been found to be inconsistent and systematically lower than the signal recorded by the two other isotopes (Vitali *et al.*, 2021). The relationship between the two water isotopes ($\delta^{18}O$ and δ^2H) in hydrological cycles is largely accepted to follow the Global Meteoric Water Line (GMWL; (Dansgaard, 1964; Voelker *et al.*, 2014). However, this O–H relationship barely holds true in the year-to-year variation of tree-ring cellulose, which exhibits site-specific patterns ranging from the expected positive relationship to negative ones (O–H relationship; Vitali *et al.*, 2021). This evidence indicates that complex interactions between hydrological and physiological components affect tree-ring cellulose $\delta^{18}O$ and δ^2H signals differently. However, disentangling the effects of these processes has proven challenging.

Recent experimental results have pointed to a different perspective for understanding the signal stored in δ^2H. Specifically, a strong link has been found between the δ^2H value of plant material and the relative proportions of autotrophic and heterotrophic processes (Yakir & Deniro, 1990; Cormier *et al.*, 2018; Cormier *et al.*, 2019). This can be explained by changes in metabolic pathways of plant leaves' carbon primary metabolism in response to climatic conditions, such as drought (Wieloch, Augusti & Schleucher, 2022; Wieloch & Grabner *et al.*, 2022), low light conditions and low CO_2 concentrations (Cormier *et al.*, 2018; Cormier *et al.*, 2019). On the other hand, changes in the δ^2H of tree-ring cellulose might also be caused by shifts in the relative use of fresh and older stored non-structural carbohydrates (NSCs) for growth, as these storage NSCs differ in their isotopic ratios (Kimak, 2015; Nabeshima *et al.*,

2018). For instance, ^{2}H-enrichment has been found under conditions where cellulose biosynthesis relies largely on NSC remobilization (e.g. earlywood, early leaf development Nabeshima *et al.*, 2018). These studies suggest the potential of $\delta^{2}H$ to be an indicator of physiological mechanisms related to the C storage dynamics of trees (Lehmann *et al.*, 2021), in addition to serving as a record of the hydrological signal from source water shared with $\delta^{18}O$ (Allen *et al.*, 2022). Therefore, a significant change in $\delta^{2}H$ values is to be expected in the case of sudden needle loss, when fresh assimilates become largely unavailable and growth has to rely on stored NSCs (Lovett *et al.*, 2002; Peters *et al.*, 2017).

In this context, defoliation events induced by insect outbreaks can be used as a non-climatic stressor, to investigate the signal recorded with $\delta^{2}H$ and the decoupling of the O–H relationship. Defoliator outbreaks induce major canopy desiccation, playing an important role in forest nutrient cycling (Berryman, 2002), but also significantly affect forest functioning and biomass production (Lovett *et al.*, 2002; Peters *et al.*, 2017). At the tree level, insect-induced defoliation events impact tree functioning by (*i*) reducing photosynthetic C uptake (Baltensweiler *et al.*, 2008), (*ii*) inducing remobilization of NSCs (Li *et al.*, 2002), and (*iii*) causing a significant decrease in soluble sugars at the leaf level (Peters *et al.*, 2020) while preserving stem and root xylem starch levels (Kosola *et al.*, 2001; Saffell *et al.*, 2014; Peters *et al.*, 2020). These results indicate the prioritization of C allocation to storage over other C-dependent processes in outbreak years (Sala *et al.*, 2012). The sum of these processes influences tree-ring cell production and therefore can be expected to induce significant shifts towards heterotrophic processes, which are reflected in the isotopic signals. Such shifts likely limit the climatic signal detectable in the isotopic signatures, in favour of non-climatic signals.

Tree-ring stable isotopes provide unique insights into the effects of insects on host tree physiology (Ulrich *et al.*, 2022). Tree-ring C isotopic ratios ($\delta^{13}C$) reflect leaf-level changes in photosynthesis and stomatal conductance, whereas oxygen isotopic ratios ($\delta^{18}O$) record changes in source water and evaporative conditions. In outbreak years, $\delta^{13}C$ values have been shown to be only slightly enriched (Ellsworth *et al.*, 1994; Haavik *et al.*, 2008; Simard *et al.*, 2008; Kress & Saurer *et al.*, 2009; Weidner *et al.*, 2010; Simard *et al.*, 2012) and $\delta^{18}O$ values only decrease slightly or show no change (Kress & Saurer *et al.*, 2009; Weidner *et al.*, 2010). Meanwhile, $\delta^{2}H$ values have been barely explored in the context of insect outbreaks.

Extensive research on larch budmoth (LBM) population outbreaks in the European Alps has yielded chronologies of both tree-ring width and maximum latewood density dating back to 800 CE (Esper *et al.*, 2007), posing a unique opportunity to further our understanding of tree physiological reactions to this non-climatic stressor and the resulting tree-ring signals. LBM infestations are caused by foliage-feeding *Lepidopteran* insects (*Zeiraphera griseana* [Hübner]). In outbreak years, LBM hatches in large quantities and feeds on needle clusters of *Larix decidua* (European larch), typically peaking by the end of June or the beginning of July (Baltensweiler *et al.*, 2008; Peters *et al.*, 2020). In this way, the mass and quality of larch foliage is reduced (Baltensweiler & Fischlin, 1988; Asshoff &

Hättenschwiler, 2006), and re-flushing may occur within 3-4 weeks of the end of larval feeding (Baltensweiler *et al.*, 2008). The feeding cycle effectively impacts the majority of the vegetative season, which spans from the start of June to the end of September. The intensity of defoliation is temporally and spatially variable, as a critical mass of larvae needs to be present to have a visible impact in an outbreak year. Further, the wave of LBM outbreaks travels across their Central European distribution (Bjørnstad *et al.*, 2002), cyclically affecting the subalpine valleys of the European Alps (Rolland *et al.*, 2001; Nola *et al.*, 2006; Esper *et al.*, 2007; Büntgen *et al.*, 2009; Kress & Saurer *et al.*, 2009; Hartl-Meier *et al.*, 2017; Saulnier *et al.*, 2017; Büntgen *et al.*, 2020). An LBM history reconstruction spanning 1200 years showed a remarkable regularity of the outbreak's recurrence, happening on average every 9 years (Esper *et al.*, 2007), and their link to cool summer temperatures (Kress & Saurer *et al.*, 2009). Climate warming has disrupted this pattern, with no extensive outbreaks occurring from the 1980s (Wermelinger & Gossner *et al.*, 2018) until 2018 when a new major outbreak occurred in Switzerland (Büntgen *et al.*, 2020). However, the interaction between LBM outbreaks and climate is still poorly understood.

This long-standing host-pathogen co-existence has indicated that larch trees cope with LBM infestations through physiological and morphological adaptations. The production of a second set of needles in the outbreak season, with traits and physiology similar to that of the first set (Peters *et al.*, 2020), comes at the expense of C reserves. Although the photosynthetic potential is restored, NSCs are not fully replenished (Wermelinger & Gossner *et al.*, 2018). The lack of C uptake due to defoliation and the use of C reserves to build the second set of needles is also reflected in a reduction in total ring width (Arbellay *et al.*, 2018). These processes result in dramatically narrower tree-ring widths and thinner latewood cell walls, which are commonly used to identify these major outbreak years (Baltensweiler *et al.*, 2008; Büntgen *et al.*, 2009; Hartl-Meier *et al.*, 2017; Arbellay *et al.*, 2018). Furthermore, these reductions have long-term effects lasting for up to 7 years (Peters *et al.*, 2017). The C-demanding cell-wall thickening process stops early during an LBM outbreak year (Peters *et al.*, 2020). Further, cell walls are thinner along the entire ring (Rolland *et al.*, 2001) and especially in the latewood (Castagneri *et al.*, 2020). The different structure of the density of outbreak rings, as shown by Castagneri *et al.* (2020), opens the question of whether annually resolved isotope measurements are suitable to investigate the impact of LBM outbreaks, as we would expect a proportionally larger share of biomass in the earlywood (EW) than in the latewood (LW). Further, in deciduous broadleaf species (*Quercus*), $\delta^{18}O$ and $\delta^{2}H$ have been shown to have lower values in LW compared with EW (Kimak, 2015; Nabeshima *et al.*, 2018). However, in deciduous conifers (Jahren & Sternberg, 2008) and for $\delta^{13}C$ (Kress & Young *et al.*, 2009) no such difference has been shown. Therefore, to answer this question separate EW and LW isotopic analyses are needed to identify whether a mass-balance issue should be accounted for in annually resolved measurements. Nonetheless, defoliator outbreaks clearly have a severe impact on trees' assimilation and allocation strategies, potentially overwriting the climatic signal. This offers the

opportunity to evaluate the "physiological signal" recorded by tree-ring isotopic ratios and δ^2H in particular.

In this study, we investigated the impact of identified LBM outbreaks on physiological signals in trees in the Swiss Lötschental valley. Specifically, we studied the signals stored in chronologies of tree-ring width, maximum latewood density, and the stable isotopes δ^2H, $\delta^{18}O$ and $\delta^{13}C$ (Esper *et al.*, 2007) in connection to the centennial changes in temperature. We investigated the following hypotheses (Hp):

1. LBM-induced changes in tree physiology create significant shifts in $\delta^{18}O$, $\delta^{13}C$ and δ^2H in tree rings.
2. LBM causes changes in the variability of intra-annual EW and LW isotopic ratios.
3. Defoliation events lead to a decoupling of the O–H relationship, due to an increase in the recorded non-climatic signal connected to the use of stored C reserves.
4. The isotopic signature in outbreak years is consistent across the seven centuries of outbreaks and is independent of temperature change.

2. Methods

2.1. Site and data sources

Both living trees and timber from buildings were pooled to construct the chronologies for this study, and a combination of published (Büntgen *et al.*, 2006; Esper *et al.*, 2007; Kress & Saurer *et al.*, 2009; Hangartner *et al.*, 2012) and unpublished data were used. The tree-ring width (TRW), maximum latewood density (MXD), $\delta^{13}C$ and $\delta^{18}O$ data utilized in this study were previously published (Büntgen *et al.*, 2006; Kress *et al.*, 2014). The *Larix decidua* Mill. samples were collected from the Lötschental, Valais, in southwestern Switzerland (46°26′N, 7°48′E). The vegetation in the sampling area is dominated by the subalpine belt of spruce-larch forests, which are gradually mixed with larch-Swiss stone pine forests towards the upper timberline, occurring at 2100 to 2200 m a.s.l. (for further details see Büntgen *et al.*, 2006 and Esper *et al.*, 2007). Samples of living trees from the same valley covered the "recent period" (1650-2004), while relict material originating from buildings in the same valley covered the "earlier period" (1256-1700; (Kress *et al.*, 2014). Both historic and living tree samples were combined into a composite chronology for further analyses (see Hangartner *et al.*, 2012). Further samples from five additional living dominant trees in the Lötschental (2000 m a.s.l., 46°23′40″N, 7°45′35″E) were used for the measurement of earlywood (EW) and latewood (LW) for selected LBM events from the 20th century or "current period" (for further details see Peters *et al.*, 2020).

2.2. LBM events

LBM defoliation events have been studied extensively to identify past outbreaks, and they correspond to severe and unambiguous alterations in the wood structure, with narrow annual tree rings containing thin latewood cell walls (Rolland *et al.*, 2001), i.e. "budmoth rings" (Baltensweiler *et al.*, 2008; Büntgen *et al.*, 2009; Hartl-Meier *et al.*, 2017; Arbellay *et al.*, 2018). For the present study, LBM events were

taken from Esper *et al.* (2007), yielding 79 events for the 1256–2004 CE (748-year) period (Table S.1). The LBM years were identified through the analysis of tree-ring density variations, and a threshold of <0.005 g cm^{-3} was set for classification as an LBM mass outbreak year (Esper *et al.*, 2007). Furthermore, we verified the identified years with field observations for several outbreaks in the 20th century by Baltensweiler *et al.* (2008) in another Swiss region (Engadin). These events were synchronised with delays of one or two years, and congruent with the spatial "wave pattern" spreading of LBM outbreaks (Bjørnstad *et al.*, 2002). Nonetheless. variation in annual TRW and MXD values in outbreak years was expected and could be attributed to variability in the intensity of outbreak events, early arrival or longer permanence of the budmoth in the years before and after the year of "critical mass" outbreak. Further, in this study, we analysed a composite chronology, which might have contributed to the variability in annual TRW and MXD values, especially in low-intensity LBM years (Esper *et al.*, 2007).

2.3. Dendrochronological methods

As reported by Kress and Saurer *et al.* (2009) and Hangartner *et al.* (2012), TRW was measured and cross-dated following standard procedures (Cook & Kairiukstis, 1990). TRW and MXD data were given as RCS-standardized chronologies (regional curve standardization, as described by Büntgen *et al.*, 2006). For isotopic analysis, five trees were selected for each period, and the cores were manually split by year using a scalpel. Each tree was analysed separately regarding the calibration period (A.D. 1900–2004). For the remaining period, all cores were pooled prior to the analysis of each annual ring, but single-tree measurements were retained every tenth year (Kress & Saurer *et al.*, 2009; Hangartner *et al.*, 2012). The first 50 years of each core were not used, to avoid any age effects from juvenile growth stages (McCarroll & Loader, 2004; Arosio *et al.*, 2020b; Arosio *et al.*, 2020a). Alpha-cellulose was extracted from all samples and isotopic ratios were measured (Filot *et al.*, 2006; Boettger *et al.*, 2007). All isotope chronologies from the different wood sources were merged and indexed according to Hangartner *et al.* (2012).

2.4. Earlywood and latewood measurements

After a 2018 LBM outbreak event, five affected trees (~200 years old) were cored in the study area at 2000 m a.s.l. (46°23′40″N, 7°45′35″E; Peters *et al.*, 2020). A core-microtome was used to obtain a plane surface suitable for TRW measurements and isotopic analysis while avoiding dust carryover between rings (Gärtner & Nievergelt, 2010). For this study, rings were dated, three years with LBM outbreaks were identified (1972, 1981, 2018), and EW and LW were visually identified and hand-split following standard procedures (Holmes, 1983). Cellulose was extracted using standard Teflon filter bags (Ankom Technology, Macedon, NY, USA), homogenized, and packed into silver capsules for the measurement of $\delta^{13}C$, $\delta^{18}O$ and $\delta^{2}H$ as described below.

2.5. Isotopic analysis

The isotope data from the long-term LBM chronologies and detailed methodological descriptions have been given in previous publications (Hangartner *et al.*, 2012; Kress *et al.*, 2014)). In brief, $\delta^{13}C$ was measured by combustion in an elemental analyser and $\delta^{18}O$ using a high-temperature pyrolysis system coupled to an isotope ratio mass spectrometer (IRMS, Delta Plus XP; Thermo Finnigan MAT, Bremen, Germany), with a precision of ca. ±0.1‰ for $\delta^{13}C$ and ±0.3‰ for $\delta^{18}O$. Corrections for past changes in the $\delta^{13}C$ of atmospheric CO_2 were applied to the raw $\delta^{13}C$ data (Leuenberger, 2007). For measuring non-exchangeable carbon-bound $\delta^{2}H$, the cellulose samples were equilibrated and subsequently converted to H_2 by high-temperature pyrolysis (TC/EA) and analysed by IRMS with a precision of ca. ±2‰ (Filot *et al.*, 2006).

For EW and LW analyses, cellulose samples were prepared and subsequently treated with the hot water-vapour equilibration method described by Schuler *et al.* (2022). In brief, samples were packed in silver capsules, equilibrated at 130°C with water of known isotopic composition for 2 hours, and dried with dry nitrogen gas for 2 h. The samples were then transferred to the autosampler of a high-temperature pyrolysis system at 60°C (PYROcube, Elementar, Hanau, Germany). The shielded autosampler was flushed with argon, and the samples were kept there for 2 h to re-equilibrate with this environment. The samples were then thermally decomposed at 1420°C and the isotopic ratios of C, O and H were measured by mass spectrometry (IRMS; Loader *et al.*, 2015; Weigt *et al.*, 2015). The hot water vapour equilibration made it possible to correct for the O-bound H isotopes (which readily exchange with water vapour and thus reflect a bias) in cellulose and to determine the non-exchangeable carbon-bound $\delta^{2}H$ (Schuler *et al.*, 2022).

2.5 Data analyses

The differences, extracted from the indexed annual chronologies, between years with LBM outbreak (event years) and those without such an event (non-event years), as well as differences between EW and LW values, were tested with the Welch t-test (Welch, 1947), which does not assume the same variance between groups. Pearson correlation matrices were used to evaluate the relationships between tree-ring parameters and to compare correlations in event and non-event years.

To compare the impact of the outbreak events across the 748-year chronology, an "event-based" normalization was carried out. For each event year, a time window of ±5 years was considered, and the values were normalized by subtracting the 5-year pre-outbreak mean (R-code adapted from Rao *et al.*, 2019). This subtraction reduces the impact of low-frequency variability, i.e. the likelihood that a cluster of low-growth years biases the classification of low or high TRW or MXD values (Adams *et al.*, 2003), and it enhances the high-frequency response signal of interest while minimizing noise. Event-based normalized data were used to investigate the effects of the 79 LBM outbreaks identified by Esper *et al.* (2007; Table S.1). A Welch t-test was performed on the normalized data ($\delta^{2}H_{norm}$, $\delta^{18}O_{norm}$, $\delta^{13}C_{norm}$) to

evaluate differences between LBM defoliation outbreak years (event years), and the 5 years prior to (pre-event years) or after the event (post-event years), singularly and as a group. $P<0.05$ was taken as the threshold of statistical significance.

The relationship between δ^2H and $\delta^{18}O$ isotopic ratios (O–H relationship) was examined with linear model fitting, for all event years and for each of the 5 years before and after outbreak years to assess any lag effect on the relationship. The century-wise linear models for the non-event years were built on a randomly selected subset of years, applying 1000 iterations to ensure a balanced sample size between the two groups (Table S.2). The century-wise linear models of event years were fitted using all event years (Table S.2).

Temperature reconstructions based on tree growth have been shown to have limitations (Wilmking *et al.*, 2020). However, they are valuable tools when alternative temperature information is not available. The temperature reconstruction used here is based on the MXD data; however, the LBM effects were regarded as noise, removed and replaced with statistical estimates (Büntgen *et al.*, 2006), showing ~60% accuracy in the validation between the reconstruction and the common period for the "recent period" (see Table 1 in Büntgen *et al.*, 2006). The summer temperature reconstruction ($T_{recon\ JJAS}$) completed by Büntgen *et al.* (2006) was used as a reference to calculate the average temperature for each century for event and non-event years (Table S.2), and their difference was tested with a two-way repeated-measures ANOVA. Century averages of $T_{recon\ JJAS}$ were then related to the slope and R^2 value of the O–H relationship to assess the impact of changing temperature on tree functioning and consequently on the isotopic signature of tree rings. All computations were performed in R version 4.0.3 (R Core Team, 2020).

3. Results

3.1. Chronologies of tree-ring parameters

The 79 LBM events described by Esper *et al.* (2007) in the indexed chronologies for tree-ring δ^2H, $\delta^{18}O$ and $\delta^{13}C$ and the RCS chronologies for TRW and MXD are presented in Fig. 1a–e. Relatively low values can be observed for $\delta^{18}O$, TRW and MXD in many outbreak years, whereas δ^2H values were generally higher than normal. The highest value in the δ^2H chronology occurred during the 1352 outbreak year. All 79 events are superimposed in Fig. 1f–l to illustrate the characteristic responses in the isotopic signatures. A significant ^2H-enrichment is clearly noticeable in the year of the event, while the 2 years after the outbreak show no significant differences from the average δ^2H values (Fig. 1f). On the contrary, ^{18}O values in outbreak years and in the first year following the outbreaks were significantly depleted compared with non-event years. $\delta^{13}C$ did not change detectably in response to outbreak years. MXD was significantly lower and TRW significantly smaller in the outbreak years and the first year following the outbreaks. The effect of outbreaks on TRW was significant up to 2 years after the events.

3.2. Earlywood and latewood differences in event years

To test whether annual isotopic ratios were potentially influenced by changes in the EW/LW mass balance, we separated EW and LW of the three most recent known budmoth outbreaks (1972, 1981, 2018), and also considered 1 year before and after each event. No significant differences were observed between EW and LW for any of the measured isotopic ratios in the year before or after an outbreak event or in the outbreak year itself (Fig. 2). δ^2H had the largest between-tree variability (maximum ±20‰) in the event year, whereas $\delta^{13}C$ and $\delta^{18}O$ had low variability (<1‰). The increase in δ^2H and decrease in $\delta^{18}O$ in LBM years observed in the overall analysis (Fig. 1) was only apparent during the outbreak in 1972.

3.3. Relationships between tree-ring parameters

In the analysis of the full chronologies, a strong correlation between $\delta^{18}O$ and $\delta^{13}C$ values was observed in both outbreak years (r=0.41) and non-event years (r=0.36; Table 1). On the contrary, the correlation between δ^2H and $\delta^{18}O$ was significantly stronger in non-event years (r= 0.50) than in outbreak years (r=0.15). This was observed to a lesser extent for the correlation between δ^2H and $\delta^{13}C$ (r=0.18 in non-event years, r=0.08 in event years). TRW was only weakly correlated with all other parameters except MXD (r=0.59). MXD was correlated similarly with $\delta^{18}O$ and $\delta^{13}C$ in non-event years (r=0.32), but poorly with δ^2H (r=0.08). In outbreak years the correlations between MXD and the other variables were much weaker.

3.4. Event-based normalization

3.4.1. Isotopic signatures

The event-based normalization involved an absolute assessment of the impact of LBM events on tree growth, independent from long-term trends, and highlighted the effects of LBM even more clearly than a simple standardization, as shown in section 3.1. In the event-based normalization, the isotopic ratios of the three elements were on average significantly different in event years compared with non-event years, with lower $\delta^{13}C_{norm}$ and $\delta^{18}O_{norm}$ and higher δ^2H_{norm} (Fig. 3).

Considering the 5 years before and after the events individually (Fig. S.1), $\delta^{18}O$ had the faster recovery to pre-event values, with only 1 year after the event being non-significantly different from the event year. Both pre-and post-event δ^2H values were significantly different from the event year, although less strongly than for $\delta^{18}O$ (Fig. S.1 a). $\delta^{13}C$ showed a prolonged effect, with less significant differences between the event year and the 5 years after (Fig. S.1 c).

The normalized values were used to further investigate the decoupling between $\delta^{18}O$ and $\delta^{2}H$ during the event and surrounding years. We observe a consistent positive relationship between $\delta^{18}O$ and $\delta^{2}H$, with the lowest strength in the event year. The 2 years after the event also show low R^2 values (~0.08), indicating a lasting effect before the system achieved a pre-disturbance balance (R^2~0.3). Further, in event years the slopes declined from ~4 to ~2, similarly indicating a loss of relationship between $\delta^{2}H$ and $\delta^{18}O$ (Figs 4, S.2).

3.4.2. Centennial temperature effect

Based on reconstructed average June to September temperatures (Büntgen *et al.*, 2006), summer temperature in LBM event years was consistently significantly lower than the century's average reconstructed temperature for all eight centuries analysed, except for the 1600s when the temperature reached an overall minimum and was not different between event and non-event years (Fig. 5). Event years and the following 2 years were consistently cooler than non-event or pre-event years.

The O–H relationship was investigated for each century in our chronology, separating the non-event years and the LBM event years, after the precautionary removal of the 2 years preceding and following the event years. The non-event years showed the expected positive relationship between $\delta^{18}O$ and $\delta^{2}H$, although the variation in the slopes and R^2 values was large (slope = 1.9 to 8, R^2 = 0.11 to 0.73; Figs 6, 7). The event years showed a wider range of O–H relationship in terms of slope and strength (slope = -4.5 to 8.9, R^2 = 0.039 to 0.82; Figs 6, 7), with negative relationships occurring in the first part of the chronology (i.e. the 1300s to 1500s) and positive relationships occurring from the 1600s to 1900s. No LBM outbreak was recorded in the 2000s.

We then compared the strengths of these correlations with the estimated average centennial temperatures (Fig. 7). Higher summer temperatures corresponded to a more positive O–H relationship in non-event years and improved the goodness-of-fit for linear regression models for each century, with a peak in the 1900s when R^2 reached 0.58, indicating a strong influence of temperature. Average summer (JJAS= June, July, August, September) temperatures did not correspond to the slope or R^2 of the O–H relationship in event years across the centuries (Fig. 7), indicating a large between-century variability in event years and a decoupling from summer temperature.

4. Discussion

This study is among the first to investigate δ^2H from tree-ring cellulose, and it demonstrates the usefulness of this parameter for assessing past physiological changes in the metabolic performance of trees. We found δ^2H changes particularly informative when considered in relation to $\delta^{18}O$, as the decoupling of the two water isotopes indicates an overwriting of the hydrological signal originating from the source water by physiological processes, with the use of stored NSCs leading to an ^{18}O-depletion and ^2H-enrichment of cellulose. The distinct processes involved in LBM outbreaks, which interfere with the recording of the climatic signal by hindering leaf-level functions and triggering resource relocation, enabled us to isolate outbreak-specific non-climatic patterns of enrichment or depletion of the stable isotopic ratios in cellulose. Here we discuss the processes which likely influence the isotopic signals stored in tree rings, from disruption of the functioning of the photosynthetic system to stimulation of the heterotrophic mechanism, resulting in loss of strength of the O–H relationship in outbreak years.

4.1. Processes modifying isotopic ratios during outbreak events

Our analyses demonstrated the consistent and significant impact of LBM outbreaks on the isotopic composition of tree-ring cellulose over the last seven centuries. Outbreak years showed ^2H-enrichment, contrasting the ^{18}O- and ^{13}C-depletion, in comparison to non-event years, confirming our **Hp1** (Figs 1, 3). Isotope patterns in the years after the outbreaks showed only minor prolonged effects and were overall not significantly different from the values in pre-event years (Figs 3, S.1). This finding indicates that relationship trends involving isotopes recovered from LBM disturbance faster than TRW and MXD, which have a shown an impact for up to 7 years after an outbreak (Peters *et al.*, 2017; Castagneri *et al.*, 2020). This suggests that the isotopic signal recorded in outbreak years is directly connected to the LBM-induced defoliation processes and can therefore be used to trace the numerous cascade effects of the defoliation outbreaks on a tree's physiological reaction as a whole. Two major processes can be related to the shift in the recorded isotopic signals: (*i*) disruption of the gas exchange mechanisms at the foliar level and (*ii*) changes in the autotrophic and heterotrophic processes (i.e. NSCs remobilization).

Regarding the first process, caterpillars perforate needle surfaces as they feed, disrupting stomatal regulatory functions and water fluxes over the course of several weeks (Kress & Saurer *et al.*, 2009; Weidner *et al.*, 2010). The disrupted tissues of the damaged needles allow a free flow of source water, which is now in direct contact with the atmosphere, resulting in higher evaporation and ultimately desiccation of the needles (Weidner *et al.*, 2010). The changes in stomatal conductance, transpiration and leaf temperature drastically affect evapotranspiration processes and thus the isotopic fractionations and enrichment levels of leaf water (Kress & Saurer *et al.*, 2009; Weidner *et al.*, 2010). The defoliation-induced changes in needle water are then transferred to the tree rings if enough carbohydrates are still produced for cell formation and assuming that $\delta^{18}O$ and δ^2H values in tree-ring cellulose are (at least partially) the result of the leaf and source-water isotopic signals (Roden & Ehleringer, 2000). However, no clear difference between LBM-affected trees and non-affected ones was observed for $\delta^{18}O$ values of

leaf assimilates over the course of the growing season (Peters *et al.*, 2020), suggesting that disruption of the gas-exchange system plays a smaller role than generally assumed. Similar investigations of δ^2H in assimilates are still lacking. On the contrary, $\delta^{13}C$ is strongly connected to even small changes in photosynthesis and stomatal conductance, which can result in a modification of the $\delta^{13}C$ in tree rings (Farquhar *et al.*, 2007; Kress & Saurer *et al.*, 2009). However, considering the loss of stomatal regulation described above, it is interesting that the changes in $\delta^{13}C$ in outbreak years were much smaller than the shifts observed for the water isotopes. This again suggests a minor impact of leaf-functioning changes on the isotopic signal recorded in tree rings (Figs 1, 3). The duration, timing and intensity of a defoliation event might play an important role in the strength of the isotopic signal; however, no significant difference in the intensity of the outbreaks was found (data not presented). Further, defoliation can occur at different stages of EW production, and if it occurs at a later growth stage it could allow a "normal-functioning" canopy signal to be recorded in the tree rings. Nevertheless, research indicates that wood production remains low after defoliation (Peters *et al.*, 2020), suggesting that regardless of the timing of the outbreak, the "budmoth rings" (Baltensweiler *et al.*, 2008; Büntgen *et al.*, 2009; Hartl-Meier *et al.*, 2017; Arbellay *et al.*, 2018) characteristic changes should be visible both in wood anatomy and isotopic ratios.

Regarding the second process, defoliation has a major and two-fold influence on the C-use strategy. First, it hinders the production of fresh assimilates, and second, it triggers reserve remobilization for the secondary flushing and formation of new needles (Baltensweiler *et al.*, 1977; Handa *et al.*, 2005; Wermelinger, Forster & Nievergelt, 2018). Further, it has previously been observed that cell production is not fully arrested during an LBM outbreak, even in strongly defoliated trees. This indicates a continuous use of reserves for tree-ring production, even though new needle production is the reserve's main sink (Peters *et al.*, 2020). It has been shown that the use of C reserves causes a ^2H-enrichment in tree-ring cellulose (Kimak *et al.*, 2015; Cormier *et al.*, 2018; Lehmann *et al.*, 2021), and it is clear that at least part of the significant ^2H-enrichment recorded during LBM outbreaks indicates processes of NSC remobilization and changes in the carbohydrate dynamics in the needles (Peters *et al.*, 2020). The depleted ^{18}O values could also partially reflect the increased use of NSCs, as metabolites become increasingly ^{18}O depleted when travelling in the stem, due to exchange with isotopically depleted water (Gessler *et al.*, 2014). On the contrary, we would have expected a ^{13}C-enrichment effect connected to the use of starch reserves (Le Roux *et al.*, 2001; Helle & Schleser, 2004), as observed for spruce budworm (Simard *et al.*, 2008). This does not seem to be the case for LBM outbreaks, but it is in line with recent leaf-level observations that gas exchange and photosynthesis drive $\delta^{13}C$ variation when post-photosynthetic ^{13}C fractionations are low, and only small differences exist between the $\delta^{13}C$ in sugars and starch reserves (Lehmann *et al.*, 2019).

To summarize, the triple isotope signatures of defoliated larch trees are the result of a mixture of the above-mentioned leaf-level processes and C-use strategies, which explains why the interpretation of the

impact of LBM on $\delta^{18}O$ and $\delta^{13}C$ variations has been ambiguous in the past (Kress & Saurer *et al.*, 2009; Weidner *et al.*, 2010). Only a minor ^{18}O-depletion in tree-ring cellulose as a result of LBM outbreaks was reported by Kress and Saurer *et al.* (2009), who studied the same chronologies as used in the present study, albeit on a shorter time scale. The authors speculated that lower temperatures influenced the source-water signal while also triggering outbreaks. However, the reliability of the $\delta^{18}O$ climatic signal during outbreak events was questioned by Weidner *et al.* (2010), who showed relatively low $\delta^{18}O$ in outbreak years. Similarly, a low impact of LBM on $\delta^{13}C$ values was observed by both Kress and Saurer *et al.* (2009) and Weidner *et al.* (2010). However, thanks to the extremely long time-scale investigated in our study (i.e. 97 outbreaks), in combination with the event-based normalization, an overall significant ^{18}O- and ^{13}C-depletion connected to outbreak years was apparent (Fig. 3). Thus, our findings support the questioning of the climatic signal recorded by tree-ring isotopes in outbreak years. Therefore, we recommend the removal of outbreak years for high-frequency climate reconstruction studies using larch.

4.2. Lack of intra-annual differences in isotopic ratios

For some deciduous species, EW ^{18}O- and ^{2}H-enrichment compared with LW has been observed and linked to post-photosynthetic processes associated with the remobilization of stored starch and a lack of fresh photo-assimilates for cellulose synthesis during the early vegetative season (Wilson *et al.*, 1978; Epstein, 1995; Kimak, 2015; Nabeshima *et al.*, 2018). These observations drove our **Hp2** that differences in isotopic ratios in LBM years could be attributed to a strong early-season remobilization bias due to the imbalance between the thickness of EW and LW (as our long-term reconstruction was based on annual tree-ring values). However, contrary to our expectations, there was no significant difference between the EW and LW isotopic ratios in event years or the pre- and post-event years for the three outbreaks in the 1900s (Fig. 4). This difference from earlier findings might be explained by the fact that most previously tested species were also deciduous angiosperm species, for which tree growth starts before leaf flush and therefore must reflect storage use (Nabeshima *et al.*, 2018). Although larch is also a deciduous conifer species, it does not appear to apply this strategy. Instead, C assimilation for the formation of tree rings happens as an overflow mechanism of the fresh assimilates of the current year, as indicated by Peters *et al.* (2020). Intra-annual $\delta^{18}O$ and $\delta^{2}H$ measurements indicated very little variation between EW and LW, suggesting that annually resolved measurements of LBM years (i.e. whole rings) are not significantly impacted by the mass-balance effect of the narrow LW. The particularly large variation during the LBM event in 1972 compared with that in 1981 and 2018 is explained by the fact that the outbreaks were characterized by different defoliation intensities (high in 1972, low in 1981 and moderate in 2018), which has been shown to dramatically impact the strength of the resulting signals stored in the tree rings (Castagneri *et al.* 2020). Further, between-tree variations in the intensity of defoliation at the same site during the same outbreak event have been observed (Peters *et al.*, 2020), and are another source of variation influencing the signal strength in average tree-ring chronologies. On the contrary, the lack of difference between $\delta^{13}C$ in EW and LW is in line with the

findings of Kress and Young *et al.* (2009), who investigated larch samples from the Lötschental treeline and attributed a lack of ^{13}C difference in EW and LW to high C turnover rates at these locations.

4.3. LBM outbreaks impact the O–H relationship

The striking outbreak-induced changes we observed in the relationship between δ^2H and $\delta^{18}O$ support our **Hp3**. They suggest that uneven shares of climatic, hydrological and physiological signals are recorded as water isotopes. In non-event years, the correlation between $\delta^{18}O$ and δ^2H was strong (r=0.5; Table 1), suggesting a coherent dominance of the hydrological signal in the tree-ring isotopic ratios. However, their correlation dropped dramatically in outbreak years (r=0.15), and the O–H relationship deteriorated significantly in the outbreak years and recovered only in the third year after the outbreaks (Fig. 4).

Given that $\delta^{18}O$ and δ^2H share the same hydrological pathways (i.e. soil water and evaporation enrichment, and temperature dependence; Iannone *et al.*, 2010), a strong connection between the isotopic ratios of the two elements in tree-ring cellulose would be expected (Dansgaard, 1964; Edwards & Fritz, 1986; Brooks *et al.*, 2010). At a continental scale, it has indeed been reported that δ^2H and $\delta^{18}O$ stored in tree-ring cellulose are correlated and reflect, at least partially, hydrological and temperature signals (Gray & Song, 1984; Saurer, Borella & Leuenberger, 1997; Vitali *et al.*, 2021; Allen *et al.*, 2022; Lehmann *et al.*, 2022). Nonetheless, recent studies showed that O and H isotopic responses of leaf water can be different due to their different sensitivity to relative humidity and the isotopic composition of water vapour (Cernusak *et al.*, 2022), which might also influence the isotopic response of plant organic matter. The O–H relationship in tree-ring cellulose has been found to be weak over 100-year chronologies for several sites across Europe, indicating both sites- and species-specific variation (Vitali *et al.*, 2021). In experimental settings, a decoupling of the two water isotopes during biochemical processes and post-photosynthetic fractionations has been observed repeatedly (Yakir & Deniro, 1990; Luo & Sternberg, 1992; Roden & Ehleringer, 2000; Cormier *et al.*, 2018; Lehmann *et al.*, 2019; Lehmann *et al.*, 2022). The opposite patterns of $\delta^{18}O$ and δ^2H in outbreak years are likely due to the imprinting of storage used during stem wood formation, with longer-term storage compounds exchanging with plant water, leading to an ^{18}O-depletion and ^2H-enrichment before cellulose synthesis. At least for $\delta^{18}O$, this would be in line with recent insights that ^{18}O-depletion occurs as a result of post-photosynthetic isotope fractionation during the transport of sugars to sink tissues and during tree-ring cellulose synthesis (Gessler *et al.*, 2014). While similar investigations have not been completed for δ^2H, there is growing evidence of additional ^2H-enrichment connected to the use of C reserves (Kimak *et al.*, 2015; Cormier *et al.*, 2018; Lehmann *et al.*, 2021). Our results of an O–H decoupling clearly support these concepts, highlighting the important impact of resource remobilization on the δ^2H signature. Further, the O–H relationship was still not fully restored during the 2 years after the outbreaks (Fig. 4), which might indicate a longer reliance of larch trees on reserves. This suggests that a larger share of the

isotopic signal can be attributed to reserve remobilization, or to trailing canopy-level defoliation-induced processes after the main outbreak year.

4.4. Centennial changes in temperature affect the O–H relationship but not in outbreak years

Our study included not only the long-term variation in environmental conditions, ranging from cooler periods associated with the Little Ice Age (1350–1850) to warmer ones in the 1900s and 2000s (Büntgen *et al.*, 2006) but also short-term temperature variation around each LBM event year. During the past seven centuries, LBM outbreaks occurred in years that were colder than non-event years (Fig. 5). As suggested by Kress and Saurer *et al.* (2009), below-average temperatures of the vegetative season peak (corresponding to July to August in the Lötschental) appear to trigger LBM outbreaks, as they aid in the synchronization of larvae development and needle maturation (Baltensweiler *et al.*, 1977; Asshoff & Hättenschwiler, 2006). Although the LBM cycle is quite regular on average, there is still variability by several years in the recurrence time, which could be related to this temperature influence (Esper *et al.*, 2007). Further, uncertainties in the identification of outbreak years should be acknowledged, as small rings with a low density could be related to climatic conditions rather than to outbreak events. Nonetheless, the overall consistent lower temperatures in outbreak years are in line with the resulting ^{18}O-depleted source water. In combination with the ^{18}O- depletion due to the use of remobilized reserves (Gessler *et al.*, 2014), ^{18}O-depleted source water could explain the strong change in the $\delta^{18}O$ signal in event years. Further, the lower temperature in LBM outbreak years could also explain the ^{13}C-depletion, which is known to decrease with higher stomatal conductance under cool conditions (Barbour *et al.*, 2004; Kress & Saurer *et al.*, 2009). On the contrary, the ^{2}H-depletion connected to cooler summer conditions appears to be lost in the $\delta^{2}H$ signal, which likely indicates a masking of the hydrological signal by metabolic processes compared with $\delta^{18}O$.

The centennial shifts in temperature over our study period were reflected in the O–H relationship of non-event years, which was strongest in warmer centuries. The slope and R^2 of the O–H relationship in non-event years clearly increased with increasing average centennial temperature (Figs 6, 7), indicating a strong coupling between the two water isotopes, ergo a clear hydrology- and evaporation-driven signal. On the contrary, temperature had no impact on the O–H relationship in LBM outbreak years, as shown by the variable and non-significant relationships between the reconstructed summer temperatures and the O–H slopes or R^2 values (Fig. 6, Table S.2). This supports our **Hp4** that the isotopic signal recorded in outbreak years is more influenced by physiological aspects that are largely independent of summer temperature.

5. Conclusions

LBM outbreaks produce a typical triple isotope signature composed of ^{18}O-depletion, ^{13}C-depletion, ^{2}H-enrichment, and an unusual decoupling between $\delta^{2}H$ and $\delta^{18}O$. Our results show that: (*i*) isotopic ratios

are sensitive indicators of the effects of defoliation and, by extension, of changes in autotrophic vs heterotrophic processes; (*ii*) non-climatic stressors cause a weakening of the hydrological relationship between the two water isotopes, and (*iii*) across the centuries the hydrological relationship between $\delta^{18}O$ and $\delta^{2}H$ is temperature-dependent except in outbreak years, indicating a loss of the climatic signal. Therefore, we conclude that when the O–H relationship is weak, the use of stored reserves contributes more to the isotopic signal. In the future, combined assessments of $\delta^{2}H$ and $\delta^{18}O$ chronologies will enable the retrospective analysis of physiological signals in long tree-ring chronologies. Such analyses will provide new information on tree functioning, especially in contexts where the climatic signal is not the main signal driving isotopic ratios, for example during defoliator outbreak events. Further, tree-ring stable isotopes have the potential to improve our understanding of tree responses to past insect outbreaks, due to their annual resolution and long chronologies, and could prove key to identifying stressors which impact NSC use.

Acknowledgements

We thank S. Klesse for the valuable discussions. We are further grateful for the discussions at the "H isotope meeting: Challenges and opportunities of using H isotopes in plants as hydrological and metabolic proxies" held at the University of Basel, Switzerland (01/04/22). We thank Melissa Dawes for her help editing the manuscript.

Funding

VV: Swiss National Science Foundation (SNSF) grant (No. 200020_182092).

RLP: SNSF grant P2BSP3_184475.

MML: SNSF Ambizione grant "TreeCarbo" (No. 179978).

KT: SNSF grant "TRoxy" (No. 200021_175888).

MS: SNSF grant (No. 182092).

Author contributions

MS, MML and VV conceptualized the study. VV carried out the analyses with support from RLP. VV and MS wrote the manuscript, which was finalized with support from all the co-authors.

Data storage

The data used in this article that has not been previously published will be stored on the EnviDat (www.envidat.ch) data portal of the Swiss Federal Institute for Forest, Snow and Landscape Research WSL.

6. References

Adams, B.J., Mann, M.E. & Ammann, C.M. (2003) Proxy evidence for an El Niño-like response to volcanic forcing. *Nature*, 426(6964), 274–278. Available from: https://doi.org/10.1038/nature02101.

Allen, S.T., Sprenger, M., Bowen, G.J. & Brooks, J.R. (2022) Spatial and Temporal Variations in Plant Source Water: O and H Isotope Ratios from Precipitation to Xylem Water. In: Siegwolf, R.T.W., Brooks, J.R., Roden, J. & Saurer, M. (Eds.) *Stable Isotopes in Tree Rings*. Springer International Publishing: Cham, pp. 501–535.

Andreu-Hayles, L., Ummenhofer, C.C., Barriendos, M., Schleser, G.H., Helle, G. & Leuenberger, M. et al. (2017) 400 Years of summer hydroclimate from stable isotopes in Iberian trees. *Climate Dynamics*, 49(1-2), 143–161. Available from: https://doi.org/10.1007/s00382-016-3332-z.

Arbellay, E., Jarvis, I., Chavardès, R.D., Daniels, L.D. & Stoffel, M. (2018) Tree-ring proxies of larch bud moth defoliation: latewood width and blue intensity are more precise than tree-ring width. *Tree Physiology*, 38(8), 1237–1245. Available from: https://doi.org/10.1093/treephys/tpy057.

Arosio, T., Ziehmer-Wenz, M.M., Nicolussi, K., Schlüchter, C. & Leuenberger, M. (2020a) Cambial-age related correlations of stable isotopes and tree-ring widths in wood samples of tree-line conifers. *Biogeosciences Discuss [preprint]*. Available from: https://doi.org/10.5194/bg-2020-406.

Arosio, T., Ziehmer-Wenz, M.M., Nicolussi, K., Schlüchter, C. & Leuenberger, M. (2020b) Larch cellulose shows significantly depleted hydrogen isotope values with respect to evergreen conifers in contrast to oxygen and carbon isotopes. *Frontiers in Earth Science*, 8. Available from: https://doi.org/10.3389/feart.2020.523073.

Asshoff, R. & Hättenschwiler, S. (2006) Changes in needle quality and larch bud moth performance in response to CO_2 enrichment and defoliation of treeline larches. *Ecological Entomology*, 31(1), 84–90. Available from: https://doi.org/10.1111/j.0307-6946.2006.00756.x.

Baltensweiler, W., Benz, G., Bovey, P. & Delucchi, V. (1977) Dynamics of larch bud moth populations. *Annual Review of Entomology*, 22(1), 79–100. Available from: https://doi.org/10.1146/annurev.en.22.010177.000455.

Baltensweiler, W. & Fischlin, A. (1988) The Larch Budmoth in the Alps. In: Berryman, A.A. (Ed.) *Dynamics of Forest Insect Populations*. Springer US: Boston, MA, pp. 331–351.

Baltensweiler, W., Weber, U.M. & Cherubini, P. (2008) Tracing the influence of larch-bud-moth insect outbreaks and weather conditions on larch tree-ring growth in Engadine (Switzerland). *Oikos*, 117(2), 161–172. Available from: https://doi.org/10.1111/j.2007.0030-1299.16117.x.

Barbour, M.M., Roden, J.S., Farquhar, G.D. & Ehleringer, J.R. (2004) Expressing leaf water and cellulose oxygen isotope ratios as enrichment above source water reveals evidence of a Péclet effect. *Oecologia*, 138(3), 426–435. Available from: https://doi.org/10.1007/s00442-003-1449-3.

Berryman, A.A. (2002) *Population cycles: The case for trophic interactions / edited by Alan Berryman*. Oxford University Press: Oxford.

Bjørnstad, O.N., Peltonen, M., Liebhold, A.M. & Baltensweiler, W. (2002) Waves of larch budmoth outbreaks in the European alps. *Science (New York, N.Y.)*, 298(5595), 1020–1023. Available from: https://doi.org/10.1126/science.1075182.

Boettger, T., Haupt, M., Knöller, K., Weise, S.M., Waterhouse, J.S. & Rinne, K.T. et al. (2007) Wood cellulose preparation methods and mass spectrometric analyses of $\delta^{13}C$, $\delta^{18}O$, and nonexchangeable $\delta^{2}H$ values in cellulose, sugar, and starch: an interlaboratory comparison. *Analytical Chemistry*, 79(12), 4603–4612. Available from: https://doi.org/10.1021/ac0700023.

Brooks, R.J., Barnard, H.R., Coulombe, R. & McDonnell, J.J. (2010) Ecohydrologic separation of water between trees and streams in a Mediterranean climate. *Nature Geoscience*, 3(2), 100–104. Available from: https://doi.org/10.1038/ngeo722.

Büntgen, U., Frank, D., Liebhold, A., Johnson, D., Carrer, M. & Urbinati, C. et al. (2009) Three centuries of insect outbreaks across the European Alps. *New Phytologist*, 182(4), 929–941. Available from: https://doi.org/10.1111/j.1469-8137.2009.02825.x.

Büntgen, U., Frank, D.C., Nievergelt, D. & Esper, J. (2006) Summer temperature variations in the European Alps, a.d. 755–2004. *Journal of Climate*, 19(21), 5606–5623. Available from: https://doi.org/10.1175/JCLI3917.1.

Büntgen, U., Liebhold, A., Nievergelt, D., Wermelinger, B., Roques, A. & Reinig, F. et al. (2020) Return of the moth: rethinking the effect of climate on insect outbreaks. *Oecologia*, 192(2), 543–552. Available from: https://doi.org/10.1007/s00442-019-04585-9.

Castagneri, D., Prendin, A.L., Peters, R.L., Carrer, M., Arx, G. von & Fonti, P. (2020) Long-term impacts of defoliator outbreaks on larch xylem structure and tree-ring biomass. *Frontiers in Plant Science*, 11, 1078. Available from: https://doi.org/10.3389/fpls.2020.01078.

Cernusak, L.A., Barbeta, A., Bush, R.T., Eichstaedt Bögelein, R., Ferrio, J.P. & Flanagan, L.B. et al. (2022) Do 2 H and 18 O in leaf water reflect environmental drivers differently? *New Phytologist*, 235(1), 41–51. Available from: https://doi.org/10.1111/nph.18113.

Cook, E.R. & Kairiukstis, L.A. (1990) *Methods of Dendrochronology: Applications in the Environmental Sciences*. Springer Science & Business Media.

Cormier, M.-A., Werner, R.A., Leuenberger, M.C. & Kahmen, A. (2019) ^{2}H-enrichment of cellulose and n-alkanes in heterotrophic plants. *Oecologia*, 189(2), 365–373. Available from: https://doi.org/10.1007/s00442-019-04338-8.

Cormier, M.-A., Werner, R.A., Sauer, P.E., Gröcke, D.R., Leuenberger, M.C. & Wieloch, T. et al. (2018) ^{2}H-fractionations during the biosynthesis of carbohydrates and lipids imprint a metabolic signal on the δ2 H values of plant organic compounds. *New Phytologist*, 218(2), 479–491. Available from: https://doi.org/10.1111/nph.15016.

Dansgaard, W. (1964) Stable isotopes in precipitation. *Tellus*, 16(4), 436–468. Available from: https://doi.org/10.3402/tellusa.v16i4.8993.

Edwards, T. & Fritz, P. (1986) Assessing meteoric water composition and relative humidity from ^{18}O and ^{2}H in wood cellulose: paleoclimatic implications for southern Ontario, Canada. *Applied Geochemistry*, 1(6), 715–723. Available from: https://doi.org/10.1016/0883-2927(86)90093-4.

Ellsworth, D.S., Tyree, M.T., Parker, B.L. & Skinner, M. (1994) Photosynthesis and water-use efficiency of sugar maple (*Acer saccharum*) in relation to pear thrips defoliation. *Tree Physiology*, 14(6), 619–632. Available from: https://doi.org/10.1093/treephys/14.6.619.

Epstein, S. (1995) The isotopic climatic records in the Alleröd-Bolling-Younger Dryas and Post-Younger Dryas events. *Global biogeochemical cycles*, 9(4), 557–563.

Esper, J., Buntgen, U., Frank, D.C., Nievergelt, D. & Liebhold, A.M. (2007) 1200 years of regular outbreaks in alpine insects. *Proceedings of the Royal Society B-Biological Sciences*, (274), 671–679.

Farquhar, G.D., Cernusak, L.A. & Barnes, B. (2007) Heavy water fractionation during transpiration. *Plant Physiology*, 143(1), 11–18. Available from: https://doi.org/10.1104/pp.106.093278.

Field, R.D., Andreu-Hayles, L., D'arrigo, R.D., Oelkers, R., Luckman, B.H. & Morimoto, D. et al. (2022) Tree-ring cellulose δ18O records similar large-scale climate influences as precipitation δ18O in the Northwest Territories of Canada. *Climate Dynamics*, 58(3-4), 759–776. Available from: https://doi.org/10.1007/s00382-021-05932-4.

Filot, M.S., Leuenberger, M., Pazdur, A. & Boettger, T. (2006) Rapid online equilibration method to determine the D/H ratios of non-exchangeable hydrogen in cellulose. *Rapid Communications in Mass Spectrometry : RCM*, 20(22), 3337–3344. Available from: https://doi.org/10.1002/rcm.2743.

Gärtner, H. & Nievergelt, D. (2010) The core-microtome: A new tool for surface preparation on cores and time series analysis of varying cell parameters. *Dendrochronologia*, 28(2), 85–92. Available from: https://doi.org/10.1016/j.dendro.2009.09.002.

Gessler, A., Ferrio, J.P., Hommel, R., Treydte, K., Werner, R.A. & Monson, R.K. (2014) Stable isotopes in tree rings: towards a mechanistic understanding of isotope fractionation and mixing processes from the leaves to the wood. *Tree Physiology*, 34(8), 796–818. Available from: https://doi.org/10.1093/treephys/tpu040.

Gray, J. & Song, S.J. (1984) Climatic implications of the natural variations of D/H ratios in tree ring cellulose. *Earth and Planetary Science Letters*, 70(1), 129–138. Available from: https://doi.org/10.1016/0012-821X(84)90216-4.

Haavik, L.J., Stephen, F.M., Fierke, M.K., Salisbury, V.B., Leavitt, S.W. & Billings, S.A. (2008) Dendrochronological parameters of northern red oak (*Quercus rubra* L. (Fagaceae)) infested with red oak borer (*Enaphalodes rufulus* (Haldeman) (Coleoptera: Cerambycidae)). *Forest Ecology and Management*, 255(5-6), 1501–1509. Available from: https://doi.org/10.1016/j.foreco.2007.11.005.

Handa, I.T., Körner, C. & Hättenschwiler, S. (2005) A test of the treeline carbon limitation hypothesis by in situ CO_2 enrichment and defoliation. *Ecology*, 86(5), 1288–1300. Available from: https://doi.org/10.1890/04-0711.

Hangartner, S., Kress, A., Saurer, M., Frank, D. & Leuenberger, M. (2012) Methods to merge overlapping tree-ring isotope series to generate multi-centennial chronologies. *Chemical Geology*, 294-295, 127–134. Available from: https://doi.org/10.1016/j.chemgeo.2011.11.032.

Hartl-Meier, C., Esper, J., Liebhold, A.M., Konter, O., Rothe, A. & Büntgen, U. (2017) Effects of host abundance on larch budmoth outbreaks in the European Alps. *Agricultural and Forest Entomology*, 19, 376–387.

Helle, G. & Schleser, G.H. (2004) Beyond CO_2-fixation by Rubisco - an interpretation of $^{13}C/^{12}C$ variations in tree rings from novel intra-seasonal studies on broad-leaf trees. *Plant, Cell and Environment*, 27(3), 367–380. Available from: https://doi.org/10.1111/j.0016-8025.2003.01159.x.

Holmes, R. (1983) Computer-Assisted Quality Control in Tree-Ring Dating and Measurement. *Tree-ring Bulletin*, 43, 51–67.

Iannone, R.Q., Romanini, D., Cattani, O., Meijer, H.A.J. & Kerstel, E.R.T. (2010) Water isotope ratio (δ^2H and $\delta^{18}O$) measurements in atmospheric moisture using an optical feedback cavity enhanced absorption laser spectrometer. *Journal of Geophysical Research*, 115(D10). Available from: https://doi.org/10.1029/2009JD012895.

Jahren, A.H. & Sternberg, L.S. (2008) Annual patterns within tree rings of the Arctic middle Eocene (ca. 45 Ma): Isotopic signatures of precipitation, relative humidity, and deciduousness. *Geology*, 36(2), 99. Available from: https://doi.org/10.1130/G23876A.1.

Kimak, A. (2015) *Tracing Physiological Processes of Long Living Tree Species and Their Response on Climate Change Using Triple Isotope Analyses*. Philosophisch-naturwissenschaftliche Fakultät der Universität Bern.

Kimak, A., Kern, Z. & Leuenberger, M. (2015) Qualitative distinction of autotrophic and heterotrophic processes at the leaf level by means of triple stable isotope (C-O-H) patterns. *Frontiers in Plant Science*, 6, 1008. Available from: https://doi.org/10.3389/fpls.2015.01008.

Kosola, K.R., Dickmann, D.I., Paul, E.A. & Parry, D. (2001) Repeated insect defoliation effects on growth, nitrogen acquisition, carbohydrates, and root demography of poplars. *Oecologia*, 129(1), 65–74. Available from: https://doi.org/10.1007/s004420100694.

Kress, A., Hangartner, S., Bugmann, H., Büntgen, U., Frank, D.C. & Leuenberger, M. et al. (2014) Swiss tree rings reveal warm and wet summers during medieval times. *Geophysical Research Letters*, 41(5), 1732–1737. Available from: https://doi.org/10.1002/2013GL059081.

Kress, A., Saurer, M., Büntgen, U., Treydte, K.S., Bugmann, H. & Siegwolf, R.T.W. (2009) Summer temperature dependency of larch budmoth outbreaks revealed by Alpine tree-ring isotope chronologies. *Oecologia*, 160(2), 353–365. Available from: https://doi.org/10.1007/s00442-009-1290-4.

Kress, A., Young, G.H., Saurer, M., Loader, N.J., Siegwolf, R.T. & McCarroll, D. (2009) Stable isotope coherence in the earlywood and latewood of tree-line conifers. *Chemical Geology*, 268(1-2), 52–57. Available from: https://doi.org/10.1016/j.chemgeo.2009.07.008.

Le Roux, X., Bariac, T., Sinoquet, H., Genty, B., Piel, C. & Mariotti, A. et al. (2001) Spatial distribution of leaf water-use efficiency and carbon isotope discrimination within an isolated tree crown. *Plant, Cell and Environment*, 24(10), 1021–1032. Available from: https://doi.org/10.1046/j.0016-8025.2001.00756.x.

Lehmann, M.M., Ghiasi, S., George, G.M., Cormier, M.-A., Gessler, A. & Saurer, M. et al. (2019) Influence of starch deficiency on photosynthetic and post-photosynthetic carbon isotope fractionations. *Journal of Experimental Botany*, 70(6), 1829–1841. Available from: https://doi.org/10.1093/jxb/erz045.

Lehmann, M.M., Schuler, P., Cormier, M.-A., Allen, S.T., Leuenberger, M. & Voelker, S. (2022) The Stable Hydrogen Isotopic Signature: From Source Water to Tree Rings. In: Siegwolf, R.T.W., Brooks, J.R., Roden, J. & Saurer, M. (Eds.) *Stable Isotopes in Tree Rings.* Springer International Publishing: Cham, pp. 331–359.

Lehmann, M.M., Vitali, V., Schuler, P., Leuenberger, M. & Saurer, M. (2021) More than climate: Hydrogen isotope ratios in tree rings as novel plant physiological indicator for stress conditions. *Dendrochronologia*, 65, 125788. Available from: https://doi.org/10.1016/j.dendro.2020.125788.

Leuenberger, M. (2007) To What Extent Can Ice Core Data Contribute to the Understanding of Plant Ecological Developments of the Past? In: Dawson, T.E. & Siegwolf, R.T.W. (Eds.) *Stable isotopes as indicators of ecological change.* Academic: Oxford, pp. 211–233.

Li, H., Hoch, G. & Körner, C. (2002) Source/sink removal affects mobile carbohydrates in *Pinus cembra* at the Swiss treeline. *Trees*, 16(4), 331–337. Available from: https://doi.org/10.1007/s00468-002-0172-8.

Loader, N.J., McCarroll, D., Gagen, M., Robertson, I. & Jalkanen, R. (2007) Extracting Climatic Information from Stable Isotopes in Tree Rings. In: Dawson, T.E. & Siegwolf, R.T.W. (Eds.) *Stable isotopes as indicators of ecological change.* Academic: Oxford, pp. 25–48.

Loader, N.J., Street-Perrott, F.A., Daley, T.J., Hughes, P.D.M., Kimak, A. & Levanič, T. et al. (2015) Simultaneous determination of stable carbon, oxygen, and hydrogen isotopes in cellulose. *Analytical Chemistry*, 87(1), 376–380. Available from: https://doi.org/10.1021/ac502557x.

Loader, N.J., Young, G.H.F., McCarroll, D., Davies, D., Miles, D. & Bronk Ramsey, C. (2020) Summer precipitation for the England and Wales region, 1201–2000 ce, from stable oxygen isotopes in oak tree rings. *Journal of Quaternary Science*, 35(6), 731–736. Available from: https://doi.org/10.1002/jqs.3226.

Lovett, G.M., Christenson, L.M., Groffman, P.M., Jones, C.G., Hart, J.E. & Mitchell, M.J. (2002) Insect defoliation and nitrogen cycling in forests: Laboratory, plot, and watershed studies indicate that most of the nitrogen released from forest foliage as a result of defoliation by insects is redistributed within the ecosystem, whereas only a small fraction of nitrogen is lost by leaching. *BioScience*, 52(4), 335–341.

Luo, Y. & Sternberg, L.D.S.L. (1992) Hydrogen and oxygen isotopic fractionation during heterotrophic cellulose synthesis. *Journal of Experimental Botany*, 43(1), 47–50. Available from: https://doi.org/10.1093/jxb/43.1.47.

McCarroll, D. & Loader, N.J. (2004) Stable isotopes in tree rings. *Quaternary Science Reviews*, 23(7-8), 771–801. Available from: https://doi.org/10.1016/j.quascirev.2003.06.017.

Nabeshima, E., Nakatsuka, T., Kagawa, A., Hiura, T. & Funada, R. (2018) Seasonal changes of δD and $\delta^{18}O$ in tree-ring cellulose of *Quercus crispula* suggest a change in post-photosynthetic processes during earlywood growth. *Tree Physiology*, 38(12), 1829–1840. Available from: https://doi.org/10.1093/treephys/tpy068.

Nola, P., Morales, M., Motta, R. & Villalba, R. (2006) The role of larch budmoth (*Zeiraphera diniana* Gn.) on forest succession in a larch (*Larix decidua* Mill.) and Swiss stone pine (*Pinus cembra* L.) stand in the Susa Valley (Piedmont, Italy). *Trees*, 20(3), 371–382. Available from: https://doi.org/10.1007/s00468-006-0050-x.

Peters, R.L., Klesse, S., Fonti, P. & Frank, D.C. (2017) Contribution of climate vs. larch budmoth outbreaks in regulating biomass accumulation in high-elevation forests. *Forest Ecology and Management*, 401, 147–158. Available from: https://doi.org/10.1016/j.foreco.2017.06.032.

Peters, R.L., Miranda, J.C., Schönbeck, L., Nievergelt, D., Fonti, M.V. & Saurer, M. et al. (2020) Tree physiological monitoring of the 2018 larch budmoth outbreak: preference for leaf recovery and carbon storage over stem wood formation in Larix decidua. *Tree Physiology*, 40(12), 1697–1711. Available from: https://doi.org/10.1093/treephys/tpaa087.

R Core Team (2020) R: A Language and Environment for Statistical Computing, Vienna, Austria. Available from: https://www.r-project.org/.

Rao, M.P., Cook, E.R., Cook, B.I., Anchukaitis, K.J., D'Arrigo, R.D. & Krusic, P.J. et al. (2019) A double bootstrap approach to Superposed Epoch Analysis to evaluate response uncertainty. *Dendrochronologia*, 55, 119–124. Available from: https://doi.org/10.1016/j.dendro.2019.05.001.

Roden, J.S. & Ehleringer, J.R. (2000) Hydrogen and oxygen isotope ratios of tree ring cellulose for field-grown riparian trees. *Oecologia*, 123(4), 481–489. Available from: https://doi.org/10.1007/s004420000349.

Rolland, C., Baltensweiler, W. & Petitcolas, V. (2001) The potential for using *Larix decidua* ring widths in reconstructions of larch budmoth (*Zeiraphera diniana*) outbreak history: dendrochronological estimates compared with insect surveys. *Trees*, 15(7), 414–424. Available from: https://doi.org/10.1007/s004680100116.

Saffell, B.J., Meinzer, F.C., Woodruff, D.R., Shaw, D.C., Voelker, S.L. & Lachenbruch, B. et al. (2014) Seasonal carbohydrate dynamics and growth in Douglas-fir trees experiencing chronic, fungal-mediated reduction in functional leaf area. *Tree Physiology*, 34(3), 218–228. Available from: https://doi.org/10.1093/treephys/tpu002.

Sakashita, W., Yokoyama, Y., Miyahara, H., Aze, T., Obrochta, S.P. & Ohyama, M. et al. (2018) Assessment of Northeastern Japan Tree-Ring Oxygen Isotopes for Reconstructing Early Summer Hydroclimate and Spring Arctic Oscillation. *Geochemistry, Geophysics, Geosystems*, 19(9), 3520–3528. Available from: https://doi.org/10.1029/2018GC007634.

Sala, A., Woodruff, D.R. & Meinzer, F.C. (2012) Carbon dynamics in trees: feast or famine? *Tree Physiology*, 32(6), 764–775. Available from: https://doi.org/10.1093/treephys/tpr143.

Sano, M., Li, Z., Murakami, Y., Jinno, M., Ura, Y. & Kaneda, A. et al. (2022) Tree ring oxygen isotope dating of wood recovered from a canal in the ancient capital of Japan. *Journal of Archaeological Science: Reports*, 45, 103626. Available from: https://doi.org/10.1016/j.jasrep.2022.103626.

Saulnier, M., Roques, A., Guibal, F., Rozenberg, P., Saracco, G. & Corona, C. et al. (2017) Spatiotemporal heterogeneity of larch budmoth outbreaks in the French Alps over the last 500 years. *Canadian Journal of Forest Research*, 47(5), 667–680. Available from: https://doi.org/10.1139/cjfr-2016-0211.

Saurer, M., Aellen, K. & Siegwolf, R. (1997) Correlating delta^{13}C and delta^{18}O in cellulose of trees. *Plant, Cell and Environment*, 20(12), 1543–1550. Available from: https://doi.org/10.1046/j.1365-3040.1997.d01-53.x.

Saurer, M., Borella, S. & Leuenberger, M. (1997) δ^{18}O of tree rings of beech (*Fagus silvatica*) as a record of δ^{18}O of the growing season precipitation. *Tellus B*, 49(1), 80–92. Available from: https://doi.org/10.3402/tellusb.v49i1.15952.

Saurer, M., Siegenthaler, U. & Schweingruber, F. (1995) The climate-carbon isotope relationship in tree rings and the significance of site conditions. *Tellus B*, 47(3), 320–330. Available from: https://doi.org/10.1034/j.1600-0889.47.issue3.4.x.

Schuler, P., Cormier, M.-A., Werner, R.A., Buchmann, N., Gessler, A. & Vitali, V. et al. (2022) A high-temperature water vapor equilibration method to determine non-exchangeable hydrogen isotope ratios of sugar, starch and cellulose. *Plant, Cell and Environment*, 45, 12–22. Available from: https://doi.org/10.1111/pce.14193.

Shestakova, T.A. & Martínez-Sancho, E. (2021) Stories hidden in tree rings: A review on the application of stable carbon isotopes to dendrosciences. *Dendrochronologia*, 65, 125789. Available from: https://doi.org/10.1016/j.dendro.2020.125789.

Simard, S., Elhani, S., Morin, H., Krause, C. & Cherubini, P. (2008) Carbon and oxygen stable isotopes from tree-rings to identify spruce budworm outbreaks in the boreal forest of Québec. *Chemical Geology*, 252(1-2), 80–87. Available from: https://doi.org/10.1016/j.chemgeo.2008.01.018.

Simard, S., Morin, H., Krause, C., Buhay, W.M. & Treydte, K. (2012) Tree-ring widths and isotopes of artificially defoliated balsam firs: A simulation of spruce budworm outbreaks in Eastern Canada. *Environmental and Experimental Botany*, 81, 44–54. Available from: https://doi.org/10.1016/j.envexpbot.2012.02.012.

834 Ulrich, D.E.M., Voelker, S., Brooks, J.R. & Meinzer, F.C. (2022) Insect and Pathogen Influences on
835 Tree-Ring Stable Isotopes. In: Siegwolf, R.T.W., Brooks, J.R., Roden, J. & Saurer, M. (Eds.) *Stable*
836 *Isotopes in Tree Rings.* Springer International Publishing: Cham, pp. 711–736.
837 Vitali, V., Martínez-Sancho, E., Treydte, K., Andreu-Hayles, L., Dorado-Liñán, I. & Gutierrez, E. et al.
838 (2021) The unknown third - Hydrogen isotopes in tree-ring cellulose across Europe. *Science of the*
839 *Total Environment*, 813, 152281. Available from: https://doi.org/10.1016/j.scitotenv.2021.152281.
840 Voelker, S.L., Brooks, J.R., Meinzer, F.C., Roden, J., Pazdur, A. & Pawelczyk, S. et al. (2014)
841 Reconstructing relative humidity from plant delta18O and deltaD as deuterium deviations from the
842 global meteoric water line. *Ecological Applications : a Publication of the Ecological Society of*
843 *America*, 24(5), 960–975. Available from: https://doi.org/10.1890/13-0988.1.
844 Weidner, K., Heinrich, I., Helle, G., Löffler, J., Neuwirth, B. & Schleser, G.H. et al. (2010)
845 Consequences of larch budmoth outbreaks on the climatic significance of ring width and stable
846 isotopes of larch. *Trees*, 24(3), 399–409. Available from: https://doi.org/10.1007/s00468-010-0421-
847 1.
848 Weigt, R.B., Bräunlich, S., Zimmermann, L., Saurer, M., Grams, T.E.E. & Dietrich, H.-P. et al. (2015)
849 Comparison of δ 18 O and δ 13 C values between tree-ring whole wood and cellulose in five species
850 growing under two different site conditions. *Rapid communications in mass spectrometry : RCM*,
851 29(23), 2233–2244. Available from: https://doi.org/10.1002/rcm.7388.
852 Welch, B.L. (1947) The generalisation of student's problems when several different population variances
853 are involved. *Biometrika*, 34(1-2), 28–35. Available from: https://doi.org/10.1093/biomet/34.1-2.28.
854 Wermelinger, B., Forster, B. & Nievergelt, D. (2018) Cycles et importance de la tordeuse du mélèze,
855 (61), 1:12.
856 Wermelinger, B., Gossner, M.M., Mathis, D.S., Trummer, D. & Rigling, A. (2018) Einfluss von Klima
857 und Baumvitalität auf den Befall von Waldföhren durch rindenbrütende Insekten. *Schweizerische*
858 *Zeitschrift fur Forstwesen*, 169(5), 251–259. Available from: https://doi.org/10.3188/szf.2018.0251.
859 Wieloch, T., Augusti, A. & Schleucher, J. (2022) Anaplerotic flux into the Calvin-Benson cycle:
860 hydrogen isotope evidence for in vivo occurrence in C3 metabolism. *New Phytologist*, 234(2), 405–
861 411. Available from: https://doi.org/10.1111/nph.17957.
862 Wieloch, T., Grabner, M., Augusti, A., Serk, H., Ehlers, I. & Yu, J. et al. (2022) Metabolism is a major
863 driver of hydrogen isotope fractionation recorded in tree-ring glucose of Pinus nigra. *New*
864 *Phytologist*, 234(2), 449–461. Available from: https://doi.org/10.1111/nph.18014.
865 Wilmking, M., van der Maaten-Theunissen, M., van der Maaten, E., Scharnweber, T., Buras, A. &
866 Biermann, C. et al. (2020) Global assessment of relationships between climate and tree growth.
867 *Global Change Biology*, 26(6), 3212–3220. Available from: https://doi.org/10.1111/gcb.15057.
868 Wilson, A.T., Grinsted, M.J. & Robinson, B.W. (1978) The possibilities of deriving past climate
869 information from stable isotope studies on tree rings. *New Zealand: DSIR Science Information*
870 *Division.*
871 Yakir, D. & Deniro, M.J. (1990) Oxygen and hydrogen isotope fractionation during cellulose
872 metabolism in *Lemna gibba* L. *Plant Physiology*, 93(1), 325–332. Available from:
873 https://doi.org/10.1104/pp.93.1.325.
874
875

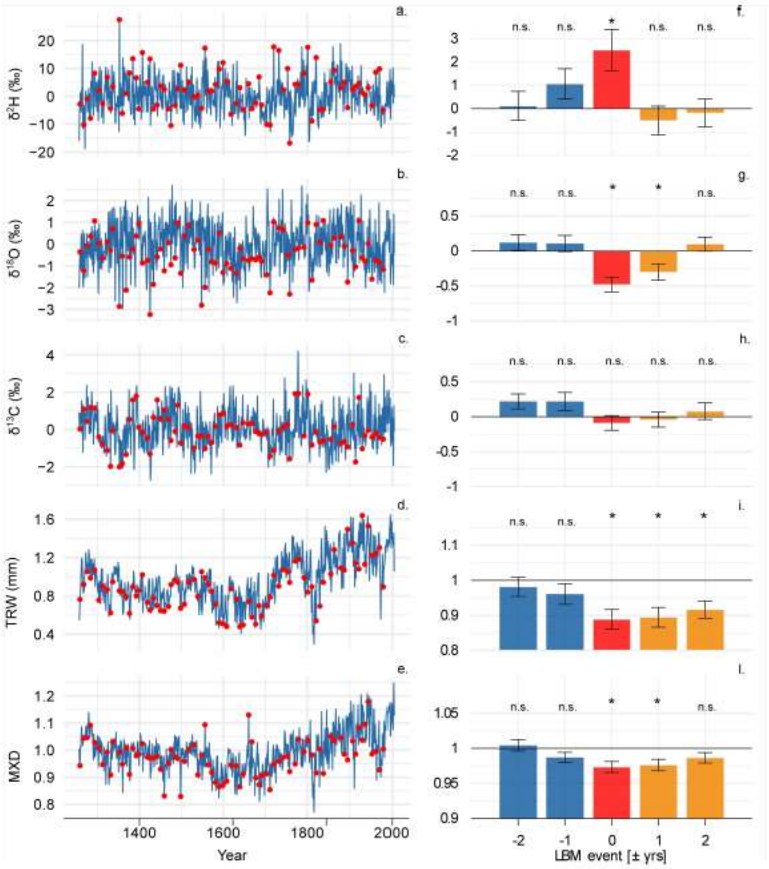

Fig. 1 (a–e) Chronologies of the tree-ring parameters δ^2H, $\delta^{18}O$, $\delta^{13}C$, tree-ring width (TRW) and indexed maximum latewood density (MXD) for the investigated period 1256–2004 (Büntgen *et al.*, 2006; Esper *et al.*, 2007; Kress & Saurer *et al.*, 2009; Hangartner *et al.*, 2012). Red dots highlight values during LBM events. (f–l) Mean LBM responses (with standard errors) of the super-imposed 79 events of tree-ring δ^2H, $\delta^{18}O$, $\delta^{13}C$, TRW index and MXD index. Significance levels were determined using a t-test comparing each variable and year around the outbreak event to 0 for the isotopes and to 1 for TRW and MXD. Blue bars represent 2 pre-event years, red bars the event year, and orange bars 2 post-event years. * P<0.05.

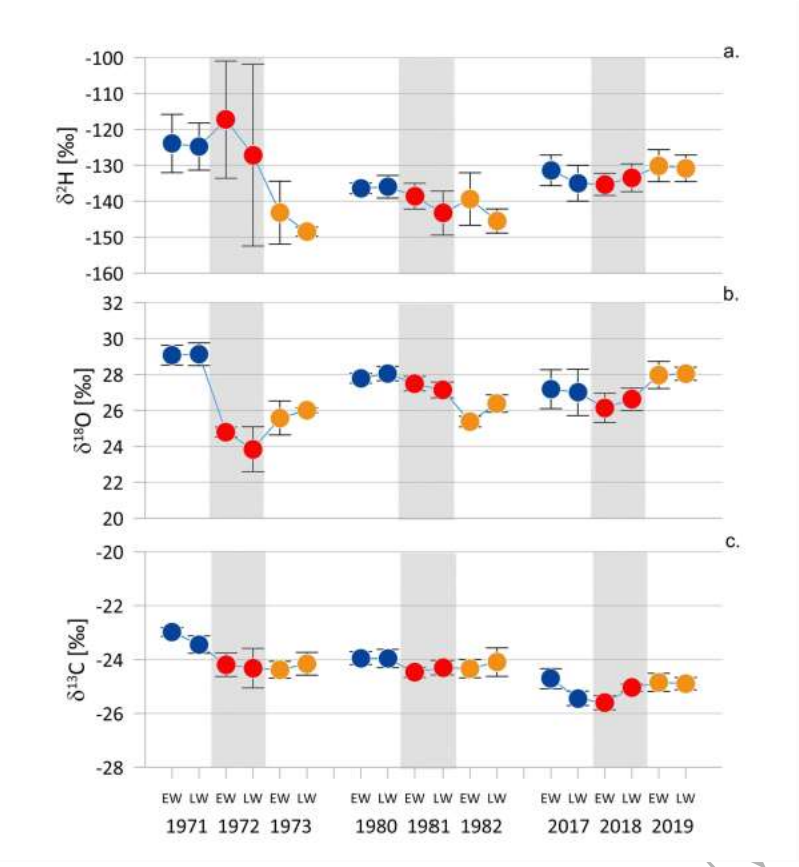

Fig. 2 Earlywood (EW) and latewood (LW) isotope values for the three measured larch budmoth outbreak events (1972, 1981, 2018; shaded areas), including the year before and after the outbreak. In each year EW and LW isotope values were not significantly different (P>0.05).

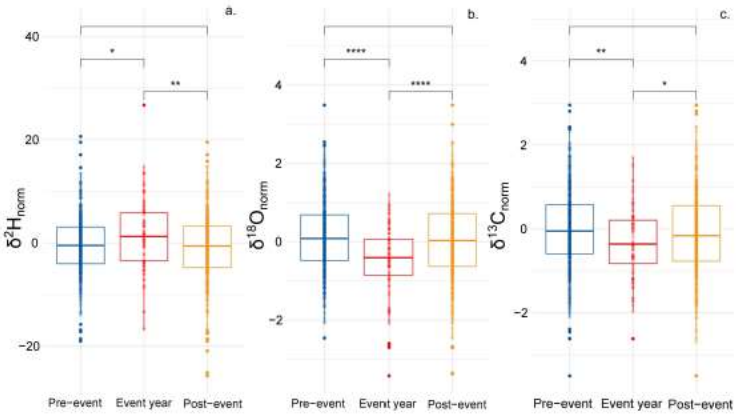

Fig. 3 Boxplots of event-based normalized differences in δ^2H, $\delta^{18}O$ and $\delta^{13}C$ between the 5 years before (pre-event years) a larch bud moth outbreak, the year of the outbreak (event year), and the 5 years after (post-event years) the outbreak, for each of the 79 larch budmoth outbreaks. Points indicate annual measurements. Significant differences between groups are indicated by asterisks (* P<0.05; ** P<0.01; *** P<0.001; **** P<0.0001).

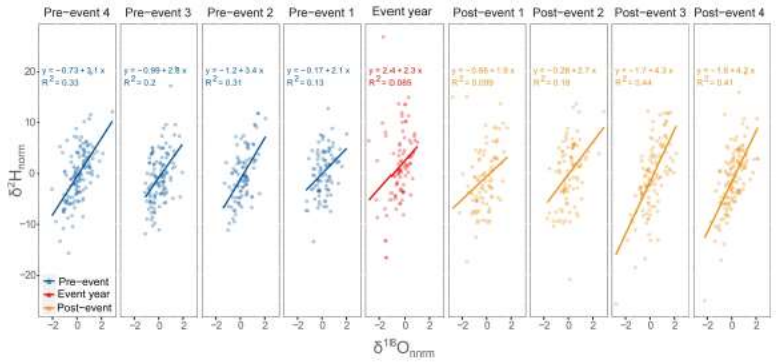

Fig. 4 Linear relationships between $\delta^{18}O_{norm}$ and $\delta^{2}H_{norm}$ in the 4 years before (pre-event) and after (post-event) each of the 79 larch budmoth outbreaks. The fitted linear model equations and explained variance (R^2) are given for each year. Colours indicate the years before or after the outbreak events. The remaining combinations of the relationships between $\delta^{18}O$ and $\delta^{13}C$ are given in the Supplementary Material (Figs S.2, S.3, S.4).

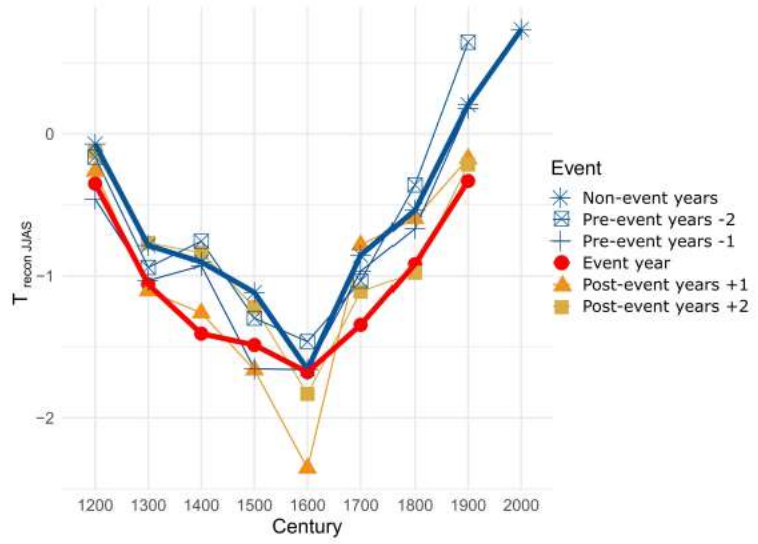

Fig. 5 Reconstructed mean summer (JJAS = June, July, August, September) temperatures for the last seven centuries (from Büntgen *et al.*, 2006), separated into event and non-event years, and ± 1 and ± 2 years around the outbreak events (pre- and post-event years). The mean summer temperature of event years was significantly different from the mean summer temperature of non-event years in the centuries 1300, 1400 and 1700.

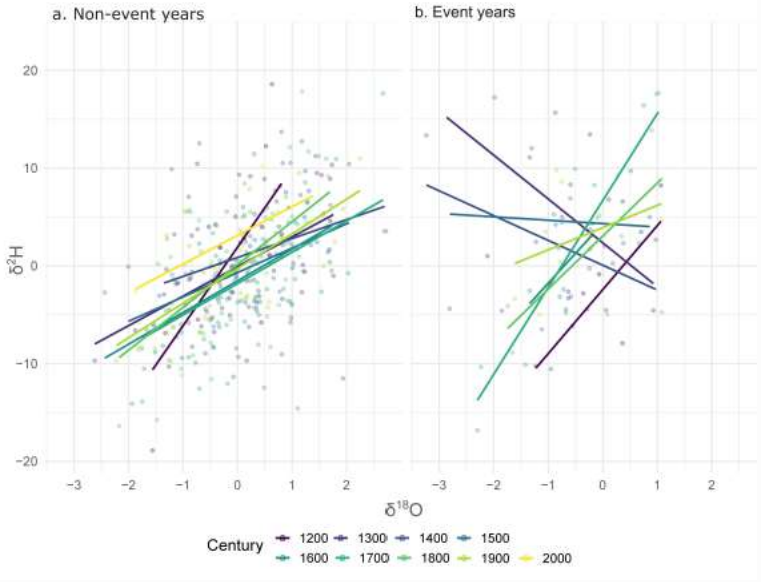

Fig. 6 O–H relationship and the respective fitted linear model for each century (indicated by different colours) for event years (a), and non-event years (b). The non-event years exclude the ±2 years around each LBM event. The equations, explained variance (R^2) and significance (P values) for the fitted linear model are given in Table S.2. No event years were recorded in the 2000s.

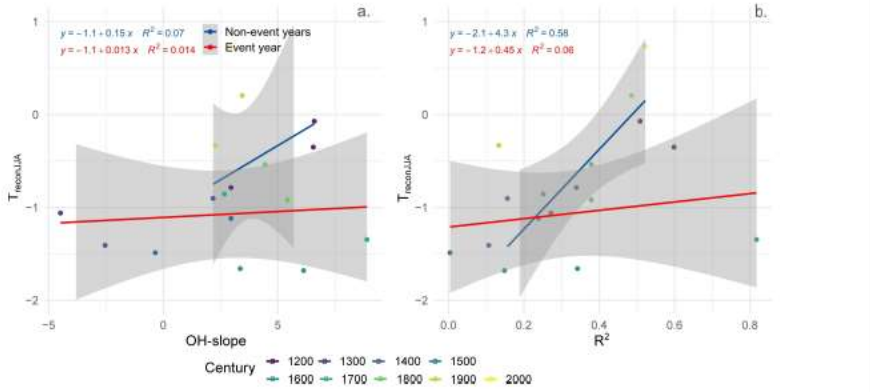

Fig. 7 O–H relationship slopes (a) and R^2 values (b) for each century in relation to the reconstructed average summer (JJAS= June, July, August, September) temperatures (from Büntgen *et al.*, 2006). For values see Table S.2.

Table 1 Pearson correlation matrices (r) between the tree-ring parameters in event years (a) and in non-event years (b) for the period 1256–2004. Significant values (a. P<0.001 if r>0.36; b. P<0.001 if r>0.16) are indicated in bold.

a. Event years

	$\delta^{18}O$	$\delta^{13}C$	$\delta^{2}H$	TRW index	MXD index
$\delta^{18}O$		**0.41**	0.15	-0.15	0.06
$\delta^{13}C$			0.08	-0.14	0.14
$\delta^{2}H$				0.07	0.14
TRW index					0.24

b. Non-event years

	$\delta^{18}O$	$\delta^{13}C$	$\delta^{2}H$	TRW index	MXD index
$\delta^{18}O$		**0.36**	**0.50**	0.16	**0.32**
$\delta^{13}C$			**0.18**	0.12	**0.32**
$\delta^{2}H$				0.01	0.08
TRW index					**0.59**

925

926

927